Local investigation of the electronic properties of size-selected Au nanoparticles by scanning tunneling spectroscopy

A. Naitabdi, L. K. Ono, and B. Roldan Cuenya[a)]
Department of Physics, University of Central Florida, Orlando, Florida 32816-2385

(Received 10 April 2006; accepted 25 May 2006; published online 24 July 2006)

The relationship between the structural/morphological and electronic properties of size-selected gold nanoparticles was investigated using scanning tunneling microscopy and spectroscopy. The nanoparticles were synthesized by inverse micelle encapsulation and were dip-coated on TiO_2/Ti(15 nm)/Si(111). Annealing in vacuum to 500 °C resulted in the removal of the polymer and the formation of an ultrathin TiC support. Significant changes in the electronic local density of states (LDOS) of the nanoparticles, in particular, the onset of nonmetallic behavior, were observed with decreasing particle size. The nanoparticle-support interactions were studied and evidence for substrate-induced modifications in the LDOS of interfacial gold atoms is found. © *2006 American Institute of Physics*. [DOI: 10.1063/1.2233601]

In the last decades the electronic, optical, magnetic, and chemical properties displayed by small metallic nanoparticles have been intensively investigated.[1–4] The recent discovery of unexpected size- and support-dependent catalytic activity of gold nanoparticles for several industrially relevant chemical reactions has awakened the interest of multiple interdisciplinary research teams in this system.[5]

Previous studies indicate that quantum size effects in small Au clusters supported on titania play a fundamental role in the structure-sensitive low temperature CO oxidation.[6,7] In addition, several other models attribute the enhanced activities observed to highly reactive gold atoms located at the nanoparticle's perimeter and to electronic charge transfer at the nanoparticle-support interface.[8,9]

This letter reports an experimental study of the electronic properties of size-selected Au nanoparticles supported on ultrathin titanium carbide films. Transition metal carbides such as TiC have shown great potential as catalytic supports due to their hardness and high melting point.[10]

By using scanning tunneling spectroscopy (STS), our work aims to get insight into how the electronic structure of the nanoparticle support can influence the local density of states (LDOS) of small Au nanoparticles.

Five commercial polystyrene-*block*-poly(2-vinylpyridine) diblock copolymers [PS(x)-*b*-P2VP(y), Polymer Source, Inc.] with different molecular weights [x/y (g/mol): 53 000/438 000, 81 000/142 000, 53 500/8800, 8200/8300, and 27 500/4300] were used to produce five-size selected Au nanoparticle systems: samples 1–5, respectively.

Following the synthesis method described in detail in Refs. 11 and 12, inverse micelles were formed by dissolving 50 mg of polymer in 10 ml of toluene. Subsequently, the gold precursor ($HAuCl_4 \cdot 3H_2O$) was added to the polymeric solution and the $AuCl_4^-$ ions were found to bond to the protonated poly(vinylpyridine) core group. The relative concentration of $HAuCl_4$ versus P2VP core was 0.6. Using this synthesis route, the size of the nanoparticles can be tuned by changing the length of the polymer core (P2VP), while the interparticle distance depends on the length of the polymer tail (PS).

Nearly hexagonally arranged, self-assembled Au nanoparticles were obtained after dip-coating the TiO_2/Ti(15 nm)/SiO_2/*n*-Si(111) substrates into the gold polymeric solution at a speed of 1 μm/min. The substrates were prepared by electron-beam evaporation of titanium on natively oxidized *n*-doped Si(111). The dip-coated substrates were then transferred to an ultrahigh vacuum system (UHV, base pressure of 1.5×10^{-10} mbar, SPECS GmbH) equipped with x-ray photoelectron spectroscopy (XPS) and scanning tunneling microscope (STM 150 Aarhus).

The samples were annealed to 500 °C for 30 min to remove the encapsulating polymers. Complete removal of the polymer from the gold nanoparticle's surface (C peak from P2VP unit) and the formation of an ultrathin TiC film were monitored using XPS.[13] After the *in situ* annealing, transmission electron microscopy (TEM) images showed the formation of multifaceted crystalline Au nanoparticles.[13]

Figure 1 displays topographic STM images of large TiC areas covered with self-assembled Au nanoparticles. The images have been ordered from top to bottom in decreasing nanoparticle size (samples 2–5). The average values of the nanoparticle heights, diameters, and interparticle distances are compiled in Table I.

In Fig. 1(a)–1(h), the homogeneous coverage and a quasihexagonal arrangement over large substrate areas of our gold nanoparticles are apparent. Such well-ordered structures take place owing to the appropriate adjustment of van der Waals interactions between the tails of the PS-P2VP diblock copolymers. Figures. 1(a) and 1(b) displays the ordered distribution of Au nanoparticles in sample 2. This system shows the largest interparticle distance, in agreement with our expectations for the encapsulating polymer with the longest tail length (PS block). Sample 3 corresponds to an intermediate size and interparticle distance [Figs. 1(c) and 1(d)]. The last two systems, samples 4 [Figs. 1(e) and 1(f)] and 5 [Figs. 1(g) and 1(h)], exhibit a high density of small Au nanoparticles (1.3–1.9 nm in height) and corroborate the preservation of the initial spatial arrangement after the removal of the polymer by a high temperature annealing treatment. Sample 1 (not shown) will be used as reference for the STS measure-

[a)]Electronic mail: roldan@physics.ucf.edu

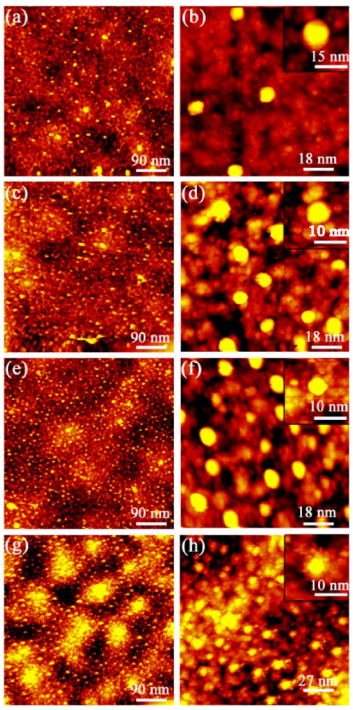

FIG. 1. (Color online) STM images of self-assembled micellar Au nanoparticles supported on thin TiC films and measured at RT after annealing in UHV to 500 °C (30 min). The scanned area on the left column was (500 $\times$ 500 nm^2) and (100 $\times$ 100 nm^2) on the right-hand side, with exception of (b) (200 $\times$ 200 nm^2) and (j) (150 $\times$ 150 nm^2). Each row corresponds to a different sample, and higher resolution images are displayed in the right column. The tunneling parameters used were I_t=0.21–1.46 nA, V_t =1.25–1.73 V. The inserts in the right column (top corner) show the nanoparticle where *I-V* curves were measured.

ments as it contains large nanoparticles with bulklike properties.

Motivated by the field of catalysis, where a relationship between the chemical reactivity of supported nanoparticles and the nature of their support has been established, a careful study of the local electronic structure of nanoparticles, support, and their interface has been carried out. Measurements of the conductance dI/dV, which at a sample bias V_s is related to the LDOS at $E-E_F=eV_s$, will contribute to the understanding of how the support-catalyst interface could contribute to the enhancement of the catalytic activity of the nanoscaled system.

Current-voltage (*I-V*) measurements on individual Au nanoparticles and ultrathin TiC films were performed in the STS mode using an etched W tip, which was systematically cleaned by Ar^+ sputtering (4.5 kV, 4.5 μA) before each acquisition. The *I-V* curves displayed in Fig. 2(a) were measured in the center of the gold nanoparticles shown in the inset of Fig. 1 (top-right corner) and on a clean TiC film obtained after *in situ* annealing a TiO_2/Ti(15 nm)/Si(111) substrate prepared in a different chamber and coated with adventitious carbon.

TABLE I. Average nanoparticle height, diameter, and interparticle distance obtained from STM images taken at room temperature after UHV annealing to 500 °C for 30 min.

Sample	Height (nm) ±0.1	Diameter (nm) ±0.1	Interparticle distance (nm) ±0.1
1	5.4	17.4	33.9
2	4.3	12.8	51.7
3	2.2	10.5	21.3
4	1.9	7.8	15.3
5	1.3	7.1	19.6

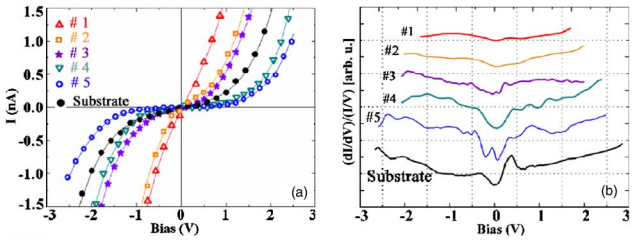

FIG. 2. (Color online) (a) STS current-voltage curves from micelle-encapsulated Au nanoparticles supported on TiC taken at room temperature after polymer removal by annealing in UHV to 500 °C. All curves were measured in the center of the respective nanoparticles. Only a selected data set and the corresponding fit have been plotted for clarity. The *I-V* curves plotted correspond to the average of 256 *I-V* curves (2 $\times$ 2 nm^2 region; samples 1, 2, and TiC) and 64 *I-V* curves (1 $\times$ 1 nm^2 region; samples 3–5) measured on top of each nanoparticle. (b) Normalized conductance calculated from the *I-V* curves displayed in (a).

The TiC substrate, Fig. 2(a) (full circles), shows a surface band gap of only 0.40±0.05 eV, which is significantly lower than the 3.2 eV obtained for a pure anatase TiO_2 substrate.[14] Since the oxygen 2*p* states populate mainly the valence-band maximum (VBM) and shift the Fermi level toward the conduction-band minimum (CBM),[15–18] the effect of annealing TiO_2 is to bring more Ti states to the VBM, where the O 2*p* levels are displaced. The Fermi level is shifted closer to these states, which then contribute more to the tunneling current. The surface band gap between the Fermi level and these states is decreased, which explains the reduced value measured for the TiC substrate.

According to the nanoparticle height, the set of *I-V* curves obtained from five different samples could be divided into two groups: samples 1 and 2 with heights of 5.2 and 4.0 nm, respectively, and samples 3–5 with heights in the range of 1.3–2.1 nm (see Table I). The *I-V* curves of samples from the first group are characterized by high tunneling currents and the conventional metallic behavior expected for bulk gold. However, a suppression of the tunneling current around zero bias (band gap) was observed in the *I-V* spectra of samples from the second size group (heigh $<$ 2 nm). Figure 2(a) demonstrates the transition from metallic to nonmetallic behavior with decreasing particle size. The largest band gaps (0.3 and 0.6 eV) were measured for the smallest nanoparticles (samples 4 and 5, respectively). This result is in agreement with a previous work conducted by Valden *et al.*[6] on UHV evaporated gold clusters supported on TiO_2(110). In analogy to that group, we attribute this behavior to size-dependent quantum size effects.

Figure. 2(b) displays the normalized conductance $(dI/dV)/(I/V)$ obtained from the *I-V* measurements in Fig. 2(a). The progressive decrease of the conductance in the zero bias region indicates a gradual electronic depletion of the nanoparticles as the height decreases. Besides, in the $(dI/dV)/(I/V)$ curve of the Au nanoparticle in sample 5 (h =1.3 nm), a broad state was observed within the band gap region. In accordance with previous studies,[19–21] we interpret this state as a defect state induced in the Au band gap by the adsorption of TiC. This feature is not observed within the reduced band gap of sample 4 (h=1.9 nm), indicating that

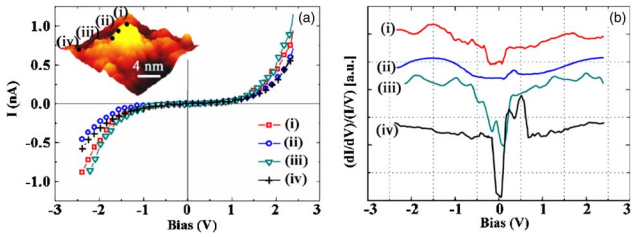

FIG. 3. (Color online) (a) STS *I-V* curves taken at different positions inside a Au nanoparticle in sample 5 [(i)–(iii)] and on the TiC support (iv). The inset in (a) shows a 3D reconstruction of the STM image corresponding to this nanoparticle (20×20 nm^2, I_t=0.22 nA, V_t=1.20 V). Only a selected data set and the corresponding fit have been plotted for clarity. The *I-V* curves plotted correspond to the average of 64 *I-V* curves taken in a 1 $\times1$ nm^2 scan region. (b) Normalized conductance calculated by numerical derivation of the *I-V* curves shown in (a).

the electronic states of the substrate are not probed at this height and that more Au states are available for tunneling in this region. Further increase in the height leads to the progressive disappearance of the band gap.

In order to get further insight into the electronic distribution within the nanoparticle and how the substrate affects its density of states, we measured local *I-V* curves at different heights within one nanoparticle in sample 5 [Fig. 3(a)].

The *I-V* curves taken inside the gold nanoparticle in sample 5 [Fig. 3(a), (i)–(iii)] confirm a height dependency in the magnitude of the band gap measured, with a minimum of 0.6 eV at the top of the nanoparticle (h=1.3 nm) and a maximum of 0.73 eV at a height of 0.66 nm. For all nanoparticle heights considered, increased tunneling currents were measured in gold as compared to the TiC substrate.

At about half of the nanoparticle's height ($h\sim0.66$ nm), [Fig. 3(b) (ii)], where a band gap of 0.73 eV was measured, only a moderate drop of the conductance was observed in the zero bias range compared to the topmost locations inside this gold nanoparticle [Fig. 3(b) (i)]. This result suggests that more states are available for tunneling due to an electronic "spillover" from the top of the nanoparticle to regions closer to the interface.

The influence of the substrate on the electronic structure of the supported Au nanoparticles becomes more evident in the normalized conductance characteristics obtained from *I-V* curves measured at the bottom of the nanoparticle [Fig. 3(b)(iii), $h\approx0.25$ nm]. Contrary to what is expected if quantum size effects are exclusively considered, for the smallest nanoparticle height at the interface with the TiC substrate, a reduced band gap (0.5 eV), as compared to higher locations within this nanoparticle, was measured. In addition, a pronounced state within the band gap at −0.15 eV is observed. This behavior indicates that electronic states from the substrate contribute to the measured LDOS. These states, together with electrons transferred from the top of the nanoparticle, lead to the enhancement of the tunneling current and hence to the decrease of the band gap measured.

Furthermore, Fig. 3(b) (iv) shows that a strong drop in the conductance of the Au-coated TiC substrate occurs in the zero bias region as compared to the uncoated substrate [Fig. 2(b)]. This points out that an electronic transfer takes place from the support to the nanoparticle.

Figure 4 compiles band gap data obtained from STS measurements on size-selected gold nanoparticles supported on ultrathin TiC films.

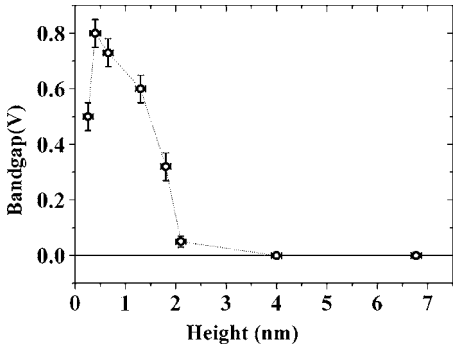

FIG. 4. Measured bandgaps as a function of the nanoparticle height.

For gold nanoparticles with heights below 2.1 nm, the monotonic increase of the band gap with decreasing nanoparticle height is evident. However, as the size is reduced below $h\sim1.3$ nm, a change in the slope (smaller band gaps) can be observed. The results from Fig. 3(b) indicate that this effect can be attributed to the contribution of states from the substrate.

In summary, this letter demonstrates that a combination of quantum size effects, electron spillover from the top of the nanoparticle to its lower boundaries, and nanoparticle-support interactions are responsible for the unusual electronic properties of small gold nanoparticles.

This work is supported by NSF (Award No. 0448491) and ACS-PRF (Award No. 42701-G5).

[1]P. Buffat and J. P. Borel, Phys. Rev. A **13**, 2287 (1976).
[2]G. K. Wertheim, S. B. DiCenzo, and S. E. Youngquist, Phys. Rev. Lett. **51**, 2310 (1983).
[3]H. G. Boyen, K. Fauth, B. Stahl, P. Ziemann, G. Kästle, F. Weigl, F. Banhart, M. Hessler, G. Schütz, N. S. Gajbhiye, J. Ellrich, H. Hahn, M. Büttner, M. G. Garnier, and P. Oelhafen, Adv. Mater. (Weinheim, Ger.) **17**, 574 (2005).
[4]M. Haruta, T. Kobayashi, H. Sano, and N. Yamada, Chem. Lett. **1987**, 405.
[5]M. Haruta, CATTECH **6**, 102 (2002).
[6]M. Valden, X. Lai, and D. W. Goodman, Science **281**, 1647 (1998).
[7]F. Cosandey and T. E. Madey, Surf. Rev. Lett. **8**, 73 (2001).
[8]M. Okumura, Y. Kitagawa, M. Haruta, and K. Yamaguchi, Appl. Catal., A **291**, 37 (2005).
[9]H. Häkkinen, S. Abbet, A. Sanchez, U. Heiz, and U. Landman, Angew. Chem., Int. Ed. **42**, 1297 (2003).
[10]Z. Chen, S. S. Perry, A. Savan, P. M. Adams, and S. V. Didziulis, J. Vac. Sci. Technol. A **23**, 234 (2005).
[11]B. Roldan Cuenya, S. H. Baeck, T. F. Jaramillo, and E. W. McFarland, J. Am. Chem. Soc. **125**, 12928 (2003).
[12]T. F. Jaramillo, S. H. Baeck, B. Roldan Cuenya, and E. W. McFarland, J. Am. Chem. Soc. **125**, 7148 (2003).
[13]L. K. Ono and B. Roldan Cuenya, Surf. Sci (submitted).
[14]J. S. Yang, D. H. Kim, S. D. Bu, T. W. Noh, S. H. Phark, Z. G. Khim, I. W. Lyo, and S. J. Oh, Appl. Phys. Lett. **82**, 3080 (2003).
[15]M. Batzill, K. Katsiev, D. J. Gaspar, and U. Diebold, Phys. Rev. B **66**, 235401 (2002).
[16]P. J. D. Lindan, N. M. Harrison, M. J. Gillan, and J. A. White, Phys. Rev. B **55**, 15919 (1997).
[17]A. T. Paxton and L. Thiên-Nga, Phys. Rev. B **57**, 1579 (1998).
[18]D. Vogtenhuber, R. Podloucky, and A. Neckel, Phys. Rev. B **49**, 2099 (1994).
[19]Zongxian Yang, Ruqian Wu, and D. W. Goodman, Phys. Rev. B **61**, 14066 (2000).
[20]R. M. Feenstra, Phys. Rev. Lett. **63**, 1412 (1989).
[21]P. Moriarty, Rep. Prog. Phys. **64**, 297 (2001).